DEVELOPMENT OF OXIDATION RESISTANT TITANIUM ALLOYS BY NIOBIUM ADDITION

DEVELOPMENT OF OXIDATION RESISTANT TITANIUM ALLOYS BY NIOBIUM ADDITION

*C. Siemers[1], F. Brunke[1], K. Saksl[2], M. Kohnke[1], G.J. Ackland[3], B. Tegner[3]

[1]*Technische Universität Braunschweig*
Institut für Werkstoffe
Langer Kamp 8
38106 Braunschweig, Germany
*(*Corresponding author: c.siemers@tu-bs.de)*

[2]*Slovak Academy of Sciences*
Institute of Materials Research
Watsonova 47
04353 Kosice, Slovak Republic

[3]*The University of Edinburgh*
School of Physics
5421 JCMB Mayfield Road
Edinburgh EH9 3JZ, United Kingdom

ABSTRACT

The application of titanium alloys is limited to 550°C due to their poor oxidation resistance. It is known that the addition of niobium improves the oxidation resistance of titanium whereas elements like vanadium do not support titanium's oxidation behaviour. Hence, the underlying mechanisms are not understood. In the present study, different binary titanium-niobium and titanium-vanadium alloys as well as commercially pure titanium were investigated. Oxidation experiments were carried out at 800°C up to 288 hours followed by metallographic analyses to study the oxide layer morphology as well as the microstructure at the interface. Energy-dispersive X-ray spectroscopy mappings (EDS) were used to identify possible changes in the distribution of the alloying elements. In addition, micro-focused hard X-ray experiments have been performed to layer-wise analyse the phase composition in selected samples. As expected, the niobium containing alloys show a better oxidation performance compared to CP-titanium and the titanium-vanadium alloys. The oxide layer consists of TiO_2 and Ti_2O_3. Depending of the niobium content, a niobium-rich layer developed below the metal-oxide-interface hindering oxygen diffusion into the titanium matrix. Based on these results, the minimal niobium content needed for improved oxidation was identified so that oxidation resistant alloys of technical relevance can be developed.

KEYWORDS

Titanium, titanium alloys, niobium, vanadium, oxidation, oxidation resistance, EDS mapping, micro-focussed hard X-ray analyses, synchrotron radiation

INTRODUCTION

Titanium belongs to the allotropic metals and can therefore exist in two different equilibrium lattice modifications. Pure titanium crystallises at 1668°C in a body centred cubic (bcc) structure called β-titanium which at 882°C transforms to a hexagonal close packed structure (hdp), the α-titanium. A martensitic β-to-α-transformation is possible at large cooling rates. This thermally induced hexagonal martensite is called the α'-phase. The transformation temperature named β-transus-temperature (T_β) can be influenced by alloying elements (Peters & Leyens, 2002).

For titanium alloy production typical alloying elements are aluminium (Al) and oxygen (O), both α-stabilisers shifting the β-transus temperature to higher temperatures, whereas tin (Sn) and zirconium (Zr) only show a limited influence on the β-transus temperature. The β-stabilising elements are subdivided into two groups: Niobium (Nb), molybdenum (Mo) and vanadium (V) stabilise the β-phase between the melting point and room temperature and are therefore called isomorphous β-stabilisers. By the addition of relatively large amounts of isomorphous β-stabilisers the β-phase can be stabilised to room temperature. Elements like chromium (Cr), copper (Cu), iron (Fe) and silicon (Si) also stabilise the β-phase to lower temperatures but undergo a eutectoid reaction during cooling. β-titanium then dissociates to α-titanium and an intermetallic compound. Consequently, these elements are called eutectoid β-stabilisers (Boyer, Welsh & Collings, 1994).

According to the phases present at room temperature, titanium alloys are divided into four main groups, namely CP-titanium (commercially pure titanium, containing low amounts of oxygen, iron, nitrogen and carbon), consisting of nearly 100% α-phase. α- and near-α-alloys are composed of α-phase and up to 5% of β-phase at room temperature. Near-β- and β-alloys on the other hand contain more than 95% of β-phase (Peters & Leyens, 2002). Finally, there are the two-phase alloys containing between 5% and 95% β-phase at room temperature. They are divided into two subgroups: In (α+β) alloys a (partial) martensitic transformation is possible, whereas in metastable β-alloys the martensite start temperature lies below room temperature. After water quenching, metastable β-alloys consist of β-phase only, the so-called supercooled metastable state (Donarchie, 1988). Ageing of supercooled β-phase leads to the formation of α-phase and the metastable ω-phase in some alloys (Ng, Douguet, Bettles & Muddle, 2010). Hence, metastable β-alloys can be precipitation hardened to ultimate tensile strengths up to 1400 MPa (Lütjering & Williams, 2007).

During the industrial titanium alloy production, titanium sponge coming from Kroll's process is mixed with alloying elements and compressed to parts (Peters & Leyens, 2002). The resulting compacts are welded together to form an electrode. The electrodes are molten to a first ingot in a vacuum arc furnace (VAR). To ensure sufficient homogeneity of the alloy, the first ingot has to be remolten once for standard applications or twice for safety critical applications, e.g. compressor discs of aircraft engines. For first ingot production, nowadays, electron beam cold hearth melting (EB-CHM) is used, especially for non-safety critical applications (Okano, Hatta, Tada & Tanaka, 2007). Independent of the melting procedure, the final ingots are normally deformed by forging, rotary swaging, rod extrusion or rolling to form bars, rods, plates or sheets (Peters & Leyens, 2002). If the thermo-mechanical treatments are performed in air, oxygen can diffuse into the surface. As oxygen is a strong α-stabiliser, a partial transformation to α-phase can occur, the so-called α-case formation. Besides the phase transformation, increased hardness, reduced toughness and notch-sensitivity are observed in the α-case due to the interstitially dissolved oxygen. Therefore, the α-case is normally removed by stripping or grinding before any application of the semi-finished products.

Titanium alloys combine a high specific fatigue strength with corrosion resistance which makes them increasingly attractive for a wide range of applications, especially in the aerospace industry in airframe and aircraft engine applications (Boyer & Williams, 2012). Much of the cost related to titanium products stems from the difficulty in reducing the oxide into a metal, but once purified, titanium is resistant to re-oxidation on account to a thin TiO_2 layer which forms spontaneously when a metallic titanium surface

is exposed to air (Fox & Yu, 2012). However, at temperatures above 550°C, this oxidation resistance is dramatically lost. This can be explained by (1) a partial transformation of Ti^{4+} ions present in TiO_2 to a mixture of Ti^{4+} and Ti^{3+} ions producing vacancies in the oxygen sub-lattice and (2) a partial transformation of TiO_2 to TiO, TiO_2 and Ti_2O_3, producing additional phase boundaries and lattice mismatches. Both effects support accelerated oxygen diffusion through the oxide layer (Lütjering & Williams, 2007). Consequently, at the metal-oxide interface, additional oxidation occurs, leading to a volume increase so that the oxide layer finally peels off and the process starts again. The poor oxidation resistance hinders the application of titanium alloys in high temperature environments, e.g. in the high pressure compressor of aircraft engines or in turbine applications, for which they are otherwise very well suited (Peters & Leyens, 2002).

Considerable efforts have been made since the late 1980ies to improve the oxidation resistance of titanium alloys at elevated temperature of both, conventional titanium alloys and titanium alumindes (Tsuyama, Mitao & Minakawa, 1992). The two most effective elements are silicon and niobium (Maki, Shioda & Sayashi, 1992). In case of silicon, this can be explained by (1) the formation of a thin SiO_2-layer at the metal-oxide interface forming a diffusion barrier for oxygen penetration and thus reducing further oxidation and (2) the precipitation of Ti_3Si intermetallic phase at the grain boundaries decelerating grain boundary oxidation (Lütjering & Williams, 2007). On the other hand, the mechanisms of niobium additions leading to improved oxidation resistance of titanium alloys are intensively discussed for several years but a satisfying, final explanation has not been found so far. Since niobium forms a pentavalent oxide, it has been believed that the effect is due to Nb^{5+} ions in the oxide. It was proposed that Nb^{5+} ions diffuse into the metal sub-lattice of the oxide (TiO_2) compensating the presence of Ti^{3+} ions which in turn trap the oxygen vacancies. Other suggested causes are the formation of Nb_2O_5 or one of the different niobium nitrides at the metal-oxide-interface, the involvement of other elements like aluminium and nitrogen, or the formation of mixed oxides (Lütjering & Willaims, 2007). Curiously, vanadium does not seem to inhibit oxide growth, although one might expect that V^{5+} ions should play a similar role to Nb^{5+}.

To examine this question, we have performed an experimental oxidation study on commercially pure titanium (CP-titanium) and different binary titanium-niobium- and titanium-vanadium-alloys. Niobium and vanadium are strong isomorphous β-stabilisers. Therefore, the amount of niobium and vanadium had to be limited to 2% (all numbers given in wt.-%) to exclude the formation of a two-phase alloy. After alloy production and a solution treatment in our laboratory furnaces, samples have been exposed to oxidation at 800°C up to 288 hours followed by metallographic analyses to study the oxide layer morphology and the microstructure as well as energy dispersive X-ray sprectroscopy (EDS) mappings in a scanning electron microscope (SEM) to identify possible changes in the niobium and vanadium distribution in the related samples. As the accuracy of EDS mappings is not sufficient to clarify the role of niobium in titanium, a micro-focused hard X-ray experiment has been carried out to layer-wise study the phase composition in a Ti 2Nb alloy oxidised for 96 hours at 800°C. The results of these experiments can now be used to develop new titanium alloys with improved oxidation behaviour.

ALLOYS, MATERIAL PRODUCTION AND EXPERIMENTS

Alloy and Sample Production

Alloy production has been carried out in a laboratory-size plasma-beam cold-hearth melter (PB-CHM). CP-Titanium Grade 2 (CP-Ti 2, O: 0.08%, Fe: 0.07%, C: 0.01%, H: 0.004%, N: 0.003%, Ti: balance, following ASTM B 348 and F 67), pure vanadium pieces (1% and 2%, purity 99.95%) and pure niobium chips (0.1%, 0.5%, 1%, 2%, purity 99.95%) were used as raw materials. Hence, the following alloys have been produced: CP-Ti 2, once remelting and casting only, Ti 1V, Ti 2V, Ti 0.1Nb, Ti 0.5Nb, Ti 1Nb and Ti 2Nb.

Contamination of the alloys during melting was minimised as the PB-CHM chamber has been evacuated twice to $2*10^{-5}$ mbar and flushed with argon (99.999%) in between. Alloy production was carried out at a pressure of 600 mbar (argon 99.999%). After melting, turning the ingot and three times

remelting, the alloys were cast into a water-cooled copper crucible so that no high-density inclusions (HDIs) were present in the cast bars of the niobium containing alloys (Siemers, Brunke, Laukart, Hussain, Rösler, Saksl, & Zahra, 2012). HDIs can occur during arc melting in case a large melting point difference of the raw materials exists. The vanadium containing alloys, therefore, do not tend to from HDIs as its melting point is close to that of titanium. The resulting round bars of diameter 13.2 mm and a length of approx. 70 mm have been stress relief annealed to release possible residual stresses form the casting process in an inert gas (argon purity 99.998%) furnace at 700°C ± 10°C for one hour followed by furnace cooling. Afterwards the bars were turned to a diameter of 12 mm to safely remove possible contaminated layers and sectioned to approx. 10 mm height by disc cutting. To ensure similar surface quality and to remove the heat affected zones, the cut faces have been ground with P800-SiC paper.

Oxidation Experiments

Oxidation experiments have been carried out in a standard furnace at 800°C ± 10°C in air for 16, 24, 48, 72, 96, 144 and 288 hours. Three samples of each alloy have been used for any individual condition. The samples were positioned in special Al_2O_3 containers with minimised contact to the metal surface so that contamination of the specimens, e.g. by chemical reactions between the metal and the crucible, could be diminished. In addition, it was ensured that even if parts of the oxide layer peeled off during the oxidation experiments all fragments were collected and scaled together with the sample to measure the accurate weight gain.

Before the oxidation experiments, the surface area of all samples has been calculated from the height and the diameter (measured at three different positions by means of a micrometre gauge, accuracy 0.01 mm). All specimens have been scaled for three times on precision scales (accuracy 0.1 mg), oxidised and afterwards rescaled to measure the weight gain during oxidation. Due to systematic errors in the volume determination, the overall accuracy of the weight gain measurements was about 10% even if the standard deviation of the individual experiments was much smaller.

Metallographic Sample Preparation and Analyses

All oxidised samples were embedded into Epomed® amorphous, glass fibre reinforced polymer by warm embedding at 180°C, 200 bar, for 10 minutes followed by water cooling. One millimetre of the embedded material has been removed by facing to eliminate the oxide layer and possible α-case (its thickness was less than 0.5 mm in any of the samples). Cross sections were prepared by water-cooled mechanical grinding with SiC grinding papers (size P240, P400, P600, P800, P1200 and P2500) and polishing (9 µm, 6 µm, 3 µm, 1 µm, Kulzer NewLam® diamond suspension including lubrication and OPS + H_2O_2 + distilled water). Finally, etching has been carried out using Kroll's reagent (6 ml HNO_3, 3 ml HF, 100 ml H_2O) for 10 to 15 seconds.

The morphology of the oxide layer and the microstructure have been analysed by means of optical microscopy (ZEISS Imager.M2m) and scanning electron microscopy (Hitachi TM 3000, LEO 1550 and FEI Helios Nanolab 650) including EDS. EDS point and line scans as well as element mappings (counting time: 1200 seconds) were carried out by means of a Bruker Quantax 70 detector to resolve possible changes in the vanadium or niobium distribution after oxidation.

Finally, one sample of Ti 2Nb alloy, oxidised for 96 hours, has been exposed to a micro-focussed hard X-ray experiment (Saksl, Rokicki, Siemers, Ostroushko, Bednarcik & Rütt, 2013) at beamline P07 at PETRA III of HASYLAB, DESY (Schell, King, Beckmann, Ruhnau, Kirchhof, Kiehn, Mueller & Schreyer, 2009). The related energy has been chosen to 84.40 keV, resulting in a wavelength of 0.01462 nm. To do so, the embedded metallographic cross-section of Ti 2Nb was shortened to 5 mm thickness by facing followed by grinding (P800) so that the metallic face of the sample was visible from both sides. This setup allowed (1) beam penetration of the sample without transmitting through the polymer and (2) the conservation of the oxide layer. After positioning the sample perpendicular to the beam by tilting the sample until a maximum photon flux of the direct beam was reached, about 80

diffraction patterns have been taken from the sample, starting at oxide layer towards the centre of the specimen. The area of exposure was 2.2 µm x 34 µm. Each pattern overlapped with the previous one by approx. 1 µm. The patterns were recorded using a Perkin Elmer 1621 detector, ten shot averaging. As a result, about 20 patterns from the oxide layer, 10 patterns from the oxide-metal-interface and 35 patterns of the base material could be analysed. The related phases have been identified using the fit2D (Hammersley, Svensson, Hanfland, Fitch & Häusermann, 1996) and CMPR (Toby, 2005) software. Only those patterns were taken into account being clearly accordable to one of the three regions.

RESULTS AND DISCUSSION

Weight Gain during Oxidation

The weight gain during oxidation of CP-Ti 2, Ti 1V, Ti 2V, Ti 1Nb and Ti 2Nb is shown in figure 1, left. The mass gain of all niobium containing alloys is presented in figure 1, right. The results have been verified by the measurement of the oxide layer thicknesses of all samples.

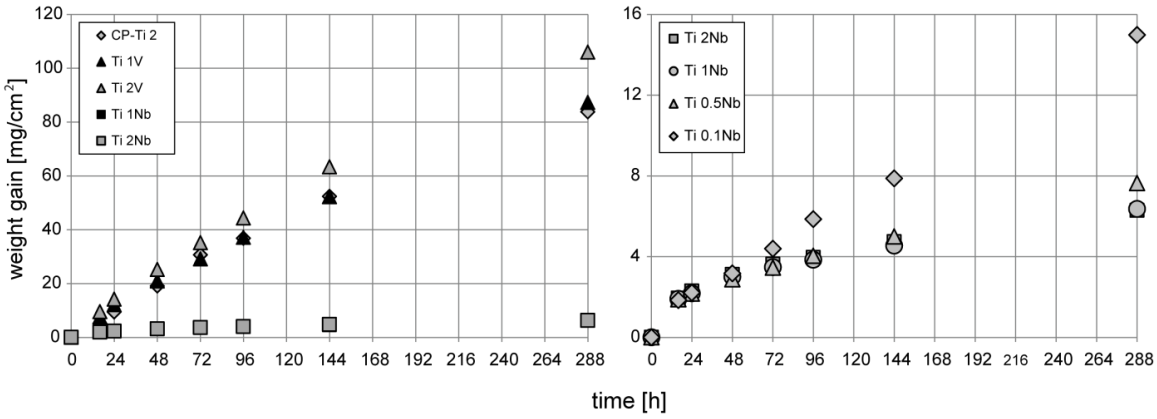

Figure 1 – Weight gain of binary titanium alloys during oxidation at 800°C up to 288 hours. Left: General overview of the oxidation behavior of CP-Ti 2, Ti 1V, Ti 2V, Ti 1Nb and Ti 2Nb. Right: Detailed analyses of the investigated Ti-Nb alloys. – Reduced oxidation is observed in all niobium containing alloys compared to CP-Ti 2 and the vanadium containing alloys.

The oxidation experiments clearly show that the presence of niobium decelerates titanium oxidation whereas the presence of vanadium led to similar oxidation behavior compared to CP-Ti 2. Even very small amounts of 0.1% niobium already improved the oxidation behavior.

In the investigated time period, CP-Ti 2, Ti 1V, Ti 2V and Ti 0.1Nb alloys showed linear weight gain over time, indicating that the oxide layer growth was not driven by diffusion whereas Ti 0.5Nb, Ti 1Nb and Ti 2Nb showed a more parabolic oxidation behavior typically observed for a diffusion-based oxidation process.

Microstructure and EDS Analyses

After melting casting and the solution treatment all investigated alloys consisted of α-phase only. The average grain size was about 100 µm. No oxide layer or α-case was visible as expected. In addition, HDIs have not been found in any of the samples.

The morphology of the oxide layers could be divided into two different groups: On the one hand, CP-Ti 2, all vanadium containing alloys as well as Ti 0.1Nb showed a layer-wise oxide growth and cracks between the layers, validating that oxygen could directly react with the metal at the metal-oxide-interface.

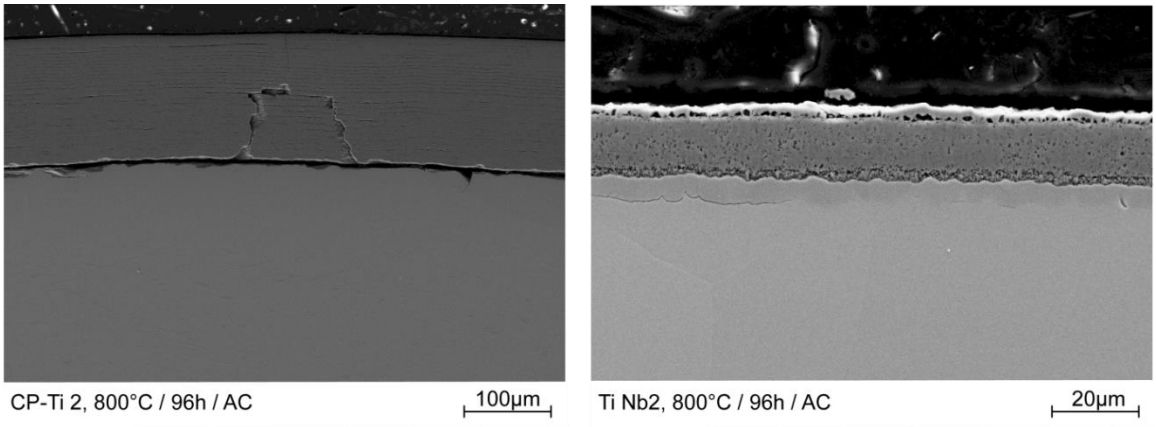

Figure 2 – Oxide layer of CP-Ti 2 (left) and Ti 2Nb (right) after 96 hours of oxidation at 800°C. The differences in the oxidation behavior as well as the additional zone in Ti 2Nb alloy at the metal-oxide-interface are clearly visible.

Hence, the oxide layer itself was not compact, see figure 2, left. This led to additional oxidation and peel-off of single layers due to an increase in volume at the interface. On the other hand, the oxide layer was compact and dense below the upper surface if a minimum amount of 0.5% of niobium was used. In addition, in these alloys, an additional zone of approx. 5 µm thickness was visible at the metal-oxide interface after 48 hours of oxidation, see figure 2, right.

At the beginning of the oxidation experiments, a homogenous niobium distribution was observed. A niobium-lean zone (the additional zone from figure 2, right) developed after approx. 48 hours of oxidation, see figure 3, left. Below the niobium-lean zone, an increased niobium content was visible in the EDS niobium mappings after an oxidation time of more than 72 hours (>1% Nb), see figure 3, right. 96 hours of oxidation were needed for the niobium-rich zone to develop if only 0.5% of niobium was added to titanium. The overall concentration of niobium in the oxide layer was below the limit of detection.

In contrast to the development of three different zones in case of the niobium containing alloys, see figure 4, left, no fluctuations in the vanadium content have been recorded in any of the vanadium containing samples after any time of oxidation, see figure 4, right.

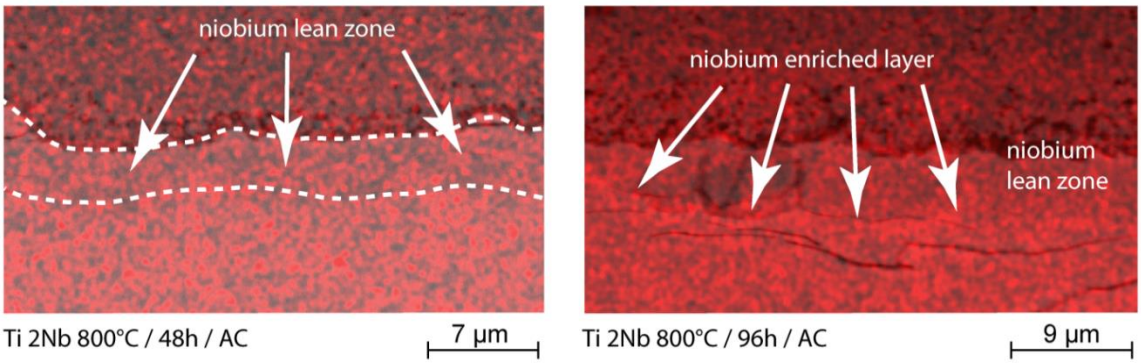

Figure 3 – Evolution of the different zones in Ti 2Nb alloy. A homogenous niobium distribution was observed in the beginning whereas a niobium-lean zone developed after 48 hours of oxidation (left). An additional niobium enriched layer was visible below the niobium-lean zone after 96 hours of oxidation (right).

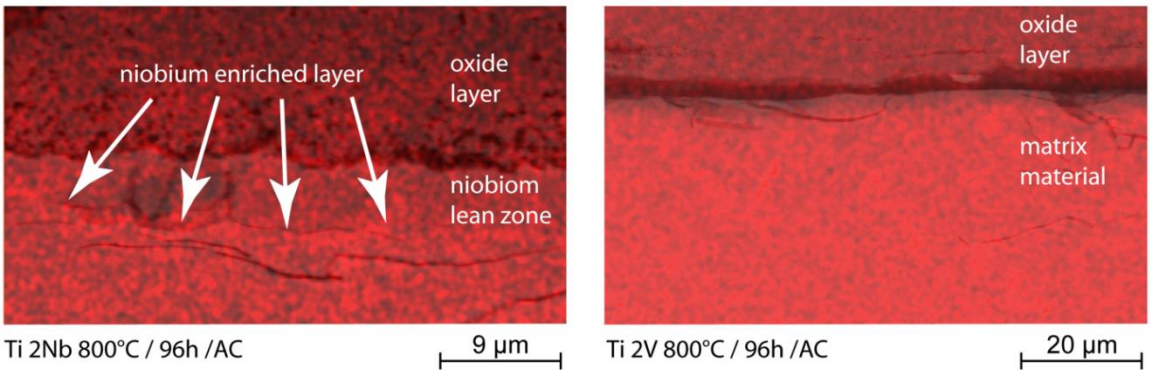

Figure 4 – Left: Niobium distribution in Ti 2Nb alloy after oxidation at 800°C for 96 hours, the white arrows mark the niobium-rich layer, verified by EDS point analyses. Right: Homogeneous vanadium distribution in Ti 2V alloy after oxidation at 800°C for 96 hours.

EDS point analyses have been carried out (diameter of the spot 2 µm, 15 spots in each zone at different positions) in the niobium-lean zone (average niobium content: 0.8% after 96 hours of oxidation. In case of Ti 2Nb alloy) and the niobium-rich (average niobium content: 2.2% after 96 hours of oxidation) zones. The matrix in this case contained 1.6% of niobium. In the vanadium containing alloys, a homogeneous average distribution of 1.7% vanadium has been measured from the bulk material to the metal-oxide-interface for Ti 2V alloy. The vanadium content in the oxide was below the limit of detection. Similar results were obtained for the other binary alloys.

Even if the systematic error in the EDS measurements is relatively large and the absolute values can differ from the measured results, the general trend is clearly traceable.

Micro-focussed Hard X-ray Experiments

The results of the micro-focussed hard X-ray experiments are presented in figure 5.

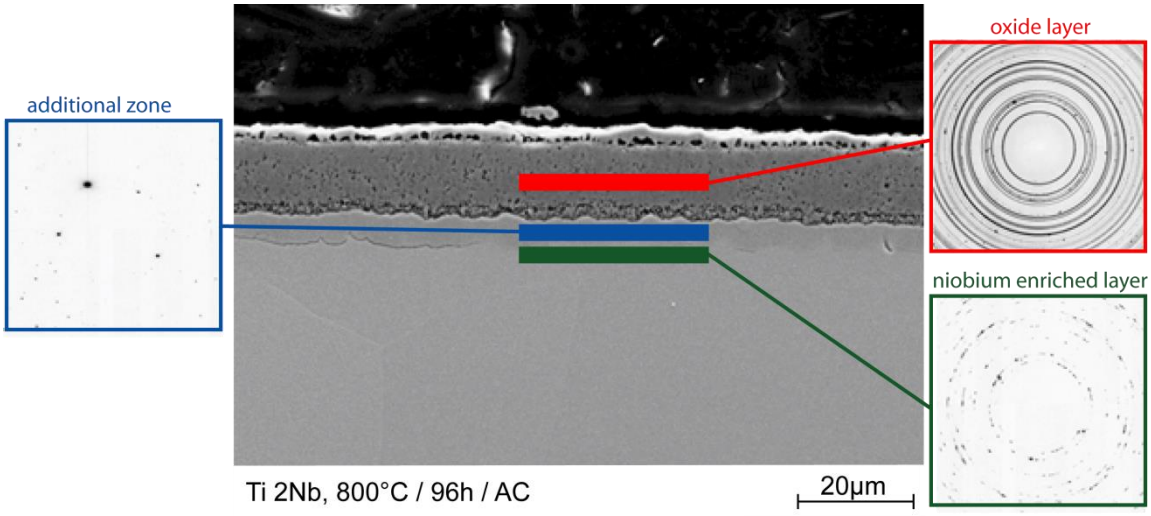

Figure 5 – Micro-focussed hard X-ray analyses from the oxide layer, the niobium-lean zone and the niobium enriched layer. The bars in the figure represent the exposure volume. Only those diffraction patterns have been taken into account clearly belonging to one of the three regions.

The analyses of the diffraction patterns include several uncertainties, e.g.: (1) the orientation of the sample to the beam might not have been absolutely perpendicular. (2) The thickness of sample leads to broadening of the peaks. (3) The diffraction patterns of the niobium-lean zone contain only a few spots so that the integration of the rings is difficult. Therefore, quantitative results cannot be presented here. Nevertheless, the following observations have been made: (1) The oxide layer consists of extremely fine-grained TiO_2 and Ti_2O_3 whereas TiO or niobium oxides and/or niobium nitrides have not been identified in the oxide layer. Related particles could only have a small volume fraction, so their peaks might be hidden in the background of the diffraction patterns. (2) The lattice parameter of TiO_2 is slightly increased compared to ideal TiO_2 indicating that niobium might be dissolved in the oxide. The lattice parameter of Ti_2O_3 is almost unchanged compared to pure Ti_2O_3. (3) Nb_2O_5 or NbN have not been identified in any of the pattern of the oxide-metal-interface, but again if a related layer is extremely thin, it might be invisible in the micro-focussed hard-X-ray experiment. (4) The niobium-lean zone consists of coarse grained α-titanium, only. The lattice parameter is slightly increased compared to pure α-titanium. EDS analyses indicated increased oxygen content in this region (α-case) compared to the metal matrix. This observation is supported by the presence of micro cracks in this area. Nevertheless, even if the niobium content is reduced here, niobium will contribute to the increase in lattice parameter as well so that a clear distinction is impossible. (5) The lattice parameter of the niobium enriched region (as identified by the EDS mappings) is increased compared to pure α-titanium and the Ti 2Nb matrix, verifying the results of the EDS mappings and point analyses.

CONCLUSIONS AND OUTLOOK

The oxidation experiments of CP-titanium as well as of different binary titanium alloys have clearly shown that niobium improves the oxidation resistance of titanium if a minimum amount of 0.5% niobium is added. In this case, the oxide layer morphology is dense and the oxide growth follows a parabolic function. The addition of vanadium does not improve the oxidation resistance of titanium alloys at all. Titanium alloys with improved oxidation resistance should, therefore, contain 0.5% niobium but no vanadium. It has to be taken into account that, on the one hand, increasing niobium contents are favourable with respect to oxidation resistance but, on the other hand, alloy production gets more difficult with increasing niobium contents as the probability of high-density inclusion formation (HDIs) is increased. From earlier investigations, the addition of 0.4% of silicon to a > 0.5% niobium containing alloy is advisable to improve the oxidation behaviour of conventional titanium alloys (Peters & Leyens, 2002).

We have discovered severe differences between the niobium and vanadium distribution during oxidation in the metal matrix of binary titanium alloys (indicating that not only the 5^+-charge of the ions is important) which can most likely be explained by the differences of the solvability of vanadium and niobium in α-titanium and their different diffusion rates in α-titanium. It is likely that vanadium can diffuse quicker into the metal matrix compared to niobium hindering the formation of a vanadium enriched layer acting as a barrier for oxygen diffusion. It is feasible if the solubility of Nb^{5+} and V^{5+} ions in TiO_2 would be different as well. To complete the picture, additional hard-X-ray analyses, especially at Ti 2V alloy, are promising.

Combined EDS- and micro-focussed hard X-ray analyses as presented here are very helpful but cannot explain whether niobium ions, vanadium ions or niobium/vanadium oxides and nitrides are present in the oxide layer at all. The question if niobium or vanadium are dissolved in the oxide layer might be investigated experimentally by wavelength dispersive X-ray spectroscopy (SEM-WDS) together with optical emission spectroscopy (ICP-OES) of the pure oxide. To do so, in future investigations, the oxide layer will be removed from the oxidised samples and separately analysed. Nevertheless, the success of such analyses strongly depends of the absolute number of dissolved foreign atoms.

Our approach has shown that the underlying mechanisms can only be fully understood by a combined simulation and experimental approach. Density functional theory (DFT) seems to be the ideal tool to analyse if alloying elements would diffuse into the oxide layer or stay in the metal, form additional oxides or nitrides or additional phases. Here, the behaviour of single foreign atoms in a titanium matrix can

be simulated which would be impossible to be detected in experimental approaches. Such simulations are planned for the near future. Their results will then be compared to and verified by the experiments to finally explain the role of niobium and vanadium in titanium alloys with respect to oxidation behaviour.

ACKNOWLEDGEMENTS

The authors thank Kai Matzigkeit from the TU Braunschweig in Braunschweig, Germany, for the oxidation experiments and Uta Ruett and Olof Gutowski for the assistance during the experiments at beamline P07 (PETRA III) of HASYLAB, DESY in Hamburg, Germany. Karel Saksl is indebted to the Slovak Grant Agency for Science for financial support (Grant No. 2/0128/13).

REFERENCES

Boyer, R., Welsh, G. & Collings, E. W., Eds. (1994). *Materials properties handbook: titanium alloys*. Ohio, USA: ASM International.

Boyer, R., Williams, J. C. (2012). Developments in Research and Applications in the Titanium Industry in the USA. In: Zhou, L., Chang, H., Lu, Y., Xu, D. (Eds.), *Twelfth World Conference on Titanium* (pp. 10-19), Beijing, China: Science Press Beijing.

Donarchie, J., Ed. (1988). *Titanium – a technical guide*. Metals Park, Ohio, USA: ASM International.

Fox, S. & Yu, K. O. (2012). Recent Changes and Developments in Titanium Extraction. In: Zhou, L., Chang, H., Lu, Y., Xu, D. (Eds.), *Twelfth World Conference on Titanium* (pp. 65-71), Beijing, China: Science Press Beijing.

Hammersley, A. P., Svensson, S. O., Hanfland, M., Fitch, A. N. & Häusermann, D. (1996). Two dimensional detector software: from real detector to idealised image or two theta scan, *High Pressure Research 14 (4-5)*, 235-248.

Lütjering, G. & Williams, J. C. (2007). *Titanium*. Berlin, Germany: Springer.

Maki, K., Shioda, M. & Sayashi, M. (1992). Effect of silicon and niobium on oxidation resistance of TiAl intermetallics, *Materials Science and Engineering: A, Volume 153 (1-2)*, 591-596.

Mitsuo, A., Uchida, S., Nihira, N., Iwaki, M. (1998). Improvement of high-temperature oxidation resistance of titanium nitride and titanium carbide films by aluminum ion implantation, *Surface and Coatings Technology, Volumes 103-104*, 98-103.

Ng, H. P., Douguet, E., Bettles, C. J. & Muddle, B.C. (2010). Age-hardening behaviour of two metastable beta-titanium alloys, *Materials Science and Engineering A 527*, 7017-7026.

Okano, H., Hatta, Y., Tada, O. & Tanaka, H. (2007). Titanium ingot production at Toho Titanium Co., Ltd. In M. Niinomi, S. Akiyama, M. Hagiwara, M. Ikeda & K. Maruyama (Eds.), *Eleventh World Conference on Titanium* (pp. 155-158), Kyoto, Japan: The Japan Institute of Metals.

Peters, M. & Leyens, C., Eds. (2002). *Titanium and titanium alloys*. Weinheim, Germany: Wiley-VCH.

Schell, N., King, A., Beckmann, F., Ruhnau, H. U., Kirchhof, R., Kiehn, R., Mueller, M. & Schreyer, A. (2009). The High Energy Materials Science Beamline (HEMS) at PETRA III. In: Garrett, R., Gentle, I., Nugent, K. & Wilkins, S (Eds.), *10th International Conference on Synchrotron Radiation Instrumentation* (pp. 391-394), Melbourne, Australia: The American Institute of Physics.

Saksl, K., Rokicki, P., Siemers, C., Ostroushko, D., Bednarcik, J. & Rütt, U. (2013). Local structure of metallic chips examined by X-ray microdiffraction, *Journal of Alloys and Compounds 581*, 579-584, DOI: 10.1016/j.jallcom.2013.07.163.

Siemers, C., Brunke, F., Laukart, J., Hussain, M. S., Rösler, J., Saksl, K. & Zahra, B. (2012), Rare Earth Metals in Titanium Alloys – A Systematic Study, in: Goode, J. R., Moldoveanu, G., & Rayat, M. S (Eds.), *Proceedings of the COM2012, Section Rare Earth Metals 2012* (pp. 281-292), Niagara Falls, Canada: The Canadian Institute of Mining, Metallurgy and Petroleum.

Toby, B. H. (2005). CMPR - a powder diffraction toolkit. *Journal of Applied Crystallography 38*, 1040-1041.

Tsuyama, S., Mitao, S. & Minakawa, K. (1992). Alloy modification of γ-base titanium aluminide for improved oxidation resistance, creep strength and fracture toughness, *Materials Science and Engineering: A, Volume 153 (1-2)*, 451-456.